Protein Science (1997), 6:304–314. Cambridge University Press. Printed in the USA.
Copyright © 1997 The Protein Society

The NMR side-chain assignments and solution structure of enzyme IIB^{cellobiose} of the phosphoenolpyruvate-dependent phosphotransferase system of *Escherichia coli*

EISO AB,[1] GEA SCHUURMAN-WOLTERS,[1] JONATHAN REIZER,[2] MILTON H. SAIER,[2] KLAAS DIJKSTRA,[1] RUUD M. SCHEEK,[1] AND GEORGE T. ROBILLARD[1]

[1]The Groningen Biomolecular Sciences and Biotechnology Institute, University of Groningen, The Netherlands
[2]Department of Biology, University of California at San Diego, La Jolla, California, 92093-0116

(RECEIVED September 18, 1996; ACCEPTED November 14, 1996)

Abstract

The assignment of the side-chain NMR resonances and the determination of the three-dimensional solution structure of the C10S mutant of enzyme IIB^{cellobiose} (IIB^{cel}) of the phosphoenolpyruvate-dependent phosphotransferase system of *Escherichia coli* are presented. The side-chain resonances were assigned nearly completely using a variety of mostly heteronuclear NMR experiments, including HCCH-TOCSY, HCCH-COSY, and COCCH-TOCSY experiments as well as CBCACOHA, CBCA(CO)NH, and HBHA(CBCA)(CO)NH experiments.

In order to obtain the three-dimensional structure, NOE data were collected from ^{15}N-NOESY-HSQC, ^{13}C-HSQC-NOESY, and 2D NOE experiments. The distance restraints derived from these NOE data were used in distance geometry calculations followed by molecular dynamics and simulated annealing protocols. In an iterative procedure, additional NOE assignments were derived from the calculated structures and new structures were calculated. The final set of structures, calculated with approximately 2000 unambiguous and ambiguous distance restraints, has an rms deviation of 1.1 Å on Cα atoms. IIB^{cel} consists of a four stranded parallel β-sheet, in the order 2134. The sheet is flanked with two and three α-helices on either side. Residue 10, a cysteine in the wild-type enzyme, which is phosphorylated during the catalytic cycle, is located at the end of the first β-strand. A loop that is proposed to be involved in the binding of the phosphoryl-group follows the cysteine. The loop appears to be disordered in the unphosphorylated state.

Keywords: ambiguous restraints; cellobiose; distance geometry; NMR; phosphocysteine; phosphoenolpyruvate-dependent phosphotransferase system; protein structure determination

Enzyme IIB^{cellobiose} (IIB^{cel}) of *Escherichia coli* is the central energy-coupling domain of the PEP-dependent phosphotransferase system for the carbohydrate cellobiose (Parker & Hall, 1990; Reizer et al., 1990). In this system, cellobiose is phosphorylated by IIB^{cel} at the expense of phospho*enol*pyruvate after transport of the sugar from the periplasmic to the cytoplasmic face of the membrane by the enzyme IIC^{cel}. Enzyme IIB^{cel} receives its phosphoryl group via a series of phosphorylation/dephosphorylation reactions involving enzyme I, HPr, and finally IIA^{cel}. For general reviews on the PEP-dependent PTS, see Meadow et al. (1990); Lolkema and Robillard (1992); Saier and Reizer (1992); Postma et al. (1993). In the case of the mannitol PTS, a conformational coupling was proposed between the phosphorylation-state of the IIB^{mtl} domain and the occurrence of facilitated diffusion through the IIC^{mtl} domain (Lolkema et al., 1991a, 1991b). *E. coli* IIB^{cel} is a protein of 106 amino acids and as such it is different from IIB-domains for most other sugars, which usually occur as constituents of multi-domain proteins. IIB^{cel} is phosphorylated at cysteine residue C10 (Pas & Robillard, 1988; Pas et al., 1988, 1991; Meins et al., 1993). The work presented here was performed on a cysteine to serine (C10S) mutant of IIB^{cel} because of expected stability problems of the wild-type protein caused by oxidation of the cysteine. Our analyses reveal that IIB^{cel} exhibits structural features similar to those that

Reprint requests to: Ruud M. Scheek, The Groningen Biomolecular Sciences and Biotechnology Institute University of Groningen, Groningen, The Netherlands; e-mail: scheek@chem.rug.nl.

Abbreviations: ^{15}N-NOESY-HSQC: 3D ^{1}H NOE ^{1}H-^{15}N heteronuclear single-quantum coherence spectroscopy; ^{15}N-TOCSY-HSQC: 3D ^{1}H total correlation ^{1}H-^{15}N heteronuclear single-quantum coherence spectroscopy; 2D NMR: two-dimensional nuclear magnetic resonance; 3D NMR: three-dimensional nuclear magnetic resonance; cel: cellobiose; DDD: distance bounds driven dynamics; EI: enzyme-I; EII: enzyme-II; EII^{glc}: enzyme-II glucose; HPr: histidine-containing protein; IIA^{cel}, IIB^{cel}, IIC^{cel}: enzyme IIA, IIB, and IIC of the cellobiose PTS (respectively); IIB^{mtl}, IIC^{mtl}: the B-domain, C-domain of enzyme-II mannitol (respectively); MD: molecular dynamics; NMR: nuclear magnetic resonance; NOE: nuclear Overhauser effect; PEP: phosphoenolpyruvate; PTPase: protein tyrosine phosphatase; PTS: phosphoenolpyruvate-dependent phosphotransferase system; mtl: mannitol; rf: radiofrequency; rmsd: root-mean-square deviation; TG: tris-acetate/glycerol; TPPI: time-proportional phase incrementation; TSP: trimethylsilylpropionic acid.

have been documented for the cysteyl-phosphorylated protein tyrosine phosphatases of eukaryotes. These latter enzymes and the enzymes IIB of the PTS are the only proteins known to involve phospho-cysteine intermediates as part of their catalytic cycle (Guan & Dixon, 1991; Cho et al., 1992).

Results

Side-chain ^1H,^{15}N, and ^{13}C assignments

The resonance assignments of nearly all backbone nuclei were obtained previously (AB et al., 1994) using double- and triple-resonance NMR spectroscopy.

Side-chain amide resonances of Asn and Gln residues were assigned by comparing NOE traces of the side-chain amide protons and backbone amide proton traces of these residues in a ^{15}N-NOESY-HSQC experiment (AB et al., 1994). Specific assignments for the cis and trans positions relative to the carboxyl oxygen were obtained from the relative intensity of the NOEs of the amide protons to the Hβ or Hγ resonances in the 2D-NOE spectrum.

The assignments for the majority of side-chain ^1H and ^{13}C resonances were obtained from the combined use of the ^{15}N-TOCSY-HSQC (AB et al., 1994), the ^{13}C-COCCH-TOCSY (E. AB, G.J.A. Kroon, K. Dijkstra, & R.M. Scheek, manuscript in preparation), the ^{13}C-HCCH-TOCSY, and the ^{13}C-HCCH-COSY, starting with knowledge of the backbone $^1H^N$, ^{15}N, $^{13}C\alpha$, ^{13}CO and $^1H\alpha$ resonance assignments.

In cases without much overlap and where, during the mixing time in the HCCH-TOCSY experiment, the ^{13}C magnetization was well distributed through the side chain, the ^{13}C and ^1H frequencies of the side-chain atoms often could be all readily assigned by inspecting the $\omega1$,$\omega2$ plane taken at the $^1H\alpha$ frequencies in $\omega3$, and the TOCSY trace taken at the $^1H\alpha$-$^{13}C\alpha$ frequencies in $\omega1$ and $\omega2$, respectively (see Fig. 1). Because there was still considerable overlap of $^1H\alpha$–$^{13}C\alpha$ frequencies, we complemented this approach by inspecting the TOCSY traces from the HCCH-TOCSY, the ^{15}N-TOCSY-HSQC, and COCCH-TOCSY experiments.

The COCCH-TOCSY experiment was especially useful in this respect. This experiment shows less overlap in the ^{13}CO,$^{13}C\alpha$ projection compared to the $^1H\alpha$,$^{13}C\alpha$ region of the HCCH-TOCSY. The ^{13}CO nuclei generally have relatively low relaxation rates and thus we could employ a relatively long constant time evolution period to obtain well-separated resonances without compromising the signal to noise ratio too much. Furthermore, like the HCCH-TOCSY, the COCCH-TOCSY uses mixing via one-bond J_{CC} couplings, which is much more effective than mixing via three-bond J_{HH} couplings as used in the ^{15}N-TOCSY-HSQC.

Approximately 90% of the side-chain proton resonances could be assigned in this manner. Geminal side-chain protons were numbered 1 and 2 in order of decreasing chemical shift.

The assignment of several, mostly long-chain residues like arginines and lysines, was difficult because of both interresidual and intraresidual overlap between β, γ, and δ resonances. The CBCACOHA, CBCA(CO)NH, and HBHA(CBCA)(CO)NH experiments were used to check the previously obtained β resonance assignments and prompted the correction of two errors where β and γ resonances were interchanged. The CBCA(CO)NH and HBHA(CBCA)(CO)NH experiments were performed using a water flip-back pulse (Grzesiek & Bax, 1993b), which returns the magnetization back to the $+Z$-axis before acquisition. This allowed for the assignment of the resonances of the backbone H^N and N nuclei of Glu 2, which were not observed in previous experiments due to rapid exchange with water.

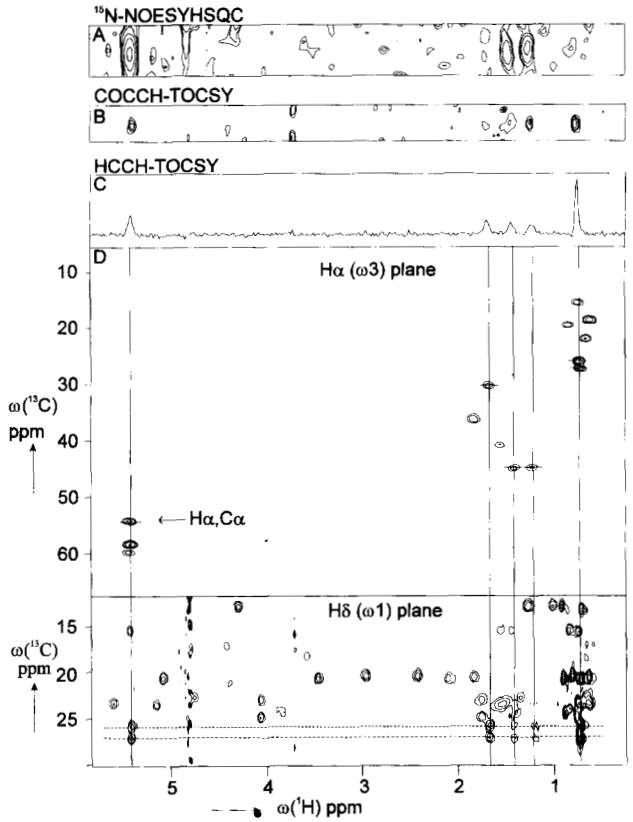

Fig. 1. Example of the strategy used for the side-chain assignment in the case of Leu 8. **A:** ^{15}N-TOCSY-HSQC trace taken at the backbone $^1H^N$, ^{15}N frequency. **B:** COCCH-TOCSY slice taken at the backbone $^{13}C\alpha$, $^{13}C'$ frequency. **C:** HCCH-TOCSY trace. **D:** HCCH-TOCSY ($\omega3$) plane taken at the $^1H\alpha$ frequency. **E:** HCCH-TOCSY ($\omega1$) plane taken at the $^1H\delta$ frequency. The $^1H\beta$ and $^1H\gamma$ frequencies are easily assigned from panels A, B, C, and D. In panel D, three possible resonances are found for the $^1H\delta$. Inspection of the TOCSY traces for these resonances in panel E, shows that the traces at 27.1 and 25.8 ppm match the TOCSY traces in panels A, B, and C.

The ^1H and ^{13}C resonances of the aromatic rings were assigned after the first round of structure determination using a ^{13}C-HCCH-TOCSY experiment tailored for the aromatic region in combination with 2D NOE data. Three of the aromatic ring systems could easily be assigned unambiguously from the NOE data alone, as they showed no interresidual NOEs with other aromatic residues. Tyr 7, Phe 9, and Phe 39, however, showed interresidual NOEs among each other and could be reliably assigned only after the first round of structure calculations.

Four sharp resonances were found in the methyl-group region of the ^{13}C-HSQC spectrum, between 1.5 and 2.0 ppm in the proton domain and between 13 and 17 ppm in the ^{13}C domain. Because these show no crosspeaks in HCCH-TOCSY experiments, they presumably belong to the methyl-groups of the four methionines in IIB^{cel}. One of these resonances was assigned to the methyl-group of Met 23 on the basis of intraresidual NOEs in the ^{13}C-HSQC-NOESY and 2D NOE spectra.

The $^1H\beta$ and $^{13}C\beta$ resonances of Ser 81 and Ser 17 were not observed in the above experiments, presumably due to overlap

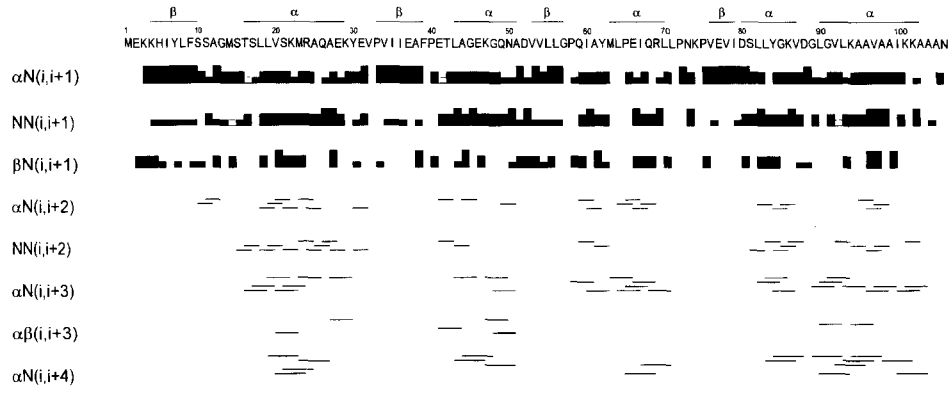

Fig. 2. Summary of short- and medium-range NOE contacts observed for IIB^{cel}. Weak, medium, and strong sequential NOEs are represented by short, medium, and long columns, respectively. Not unambiguously assigned contacts are indicated by open columns.

with the α resonances since these resonances were easily observed for the other serines. A 3D-HCH experiment (Yamazaki et. al., 1993), which shows only the methylene groups, was performed to overcome this uncertainty. Indeed, resonances were found at the expected frequencies, but the assignments for the Hβ and Cβ resonances of S81 and S17 in Table 1 remain tentative due to interresidual overlap.

The guanidinium group Hϵ and Nϵ resonances of Arg 24 and Arg 69 were assigned from their typical ^{15}N chemical shift value, in combination with 2D NOE and 3D ^{15}N-NOESY-HSQC experiments. The Hη21 of Arg 24 was assigned from the 750 MHz 2D NOE alone. From the fact that the Hϵ of Arg 24 shows weak and medium-size NOE crosspeaks to the α proton of Ile 35 and the α, the amide, and the side-chain methyl-group protons of Ile 36, together with analysis of the structures, it was inferred that this proton forms a hydrogen bond with the backbone oxygen of Ile 36.

A unique resonance frequency in the 750 MHz 2D-NOE spectrum at 6.05 ppm was assigned to the Thr 42 Hγ1 hydroxyl proton, because crosspeaks were observed with the resonances of every proton of Thr 42. All assigned chemical shift values are listed in Table 1.

NOE intensities to be used for the construction of distance restraints were collected from a 2D NOE buildup series. ^{15}N-NOESY-HSQC and ^{13}C-HSQC-NOESY experiments were used to resolve assignment ambiguities in the 2D NOE.

Short and medium range NOE contacts are summarized in Figure 2. Analysis of these NOEs together with $^{1}H\alpha$, $^{13}C\alpha$, and ^{13}CO secondary shift values (AB et al., 1994) lead to the assignment of five α-helices, residue 16–29, 43–51, 63–70, 80–87, and 90–103. Four parallel β-strands, residues 4–10, 34–39, 53–57, and 76–79, were identified on the basis of short-range NOEs, long-range interstrand H^{N}-Hα NOEs and secondary shift data. The secondary structure elements are indicated in Figure 2.

The final set of 32 structures was calculated using 50 H-bond restraints (Table 2) and 2129 NOE-based distance restraints, of which 811 were unambiguous. Of the 32 structures, 17 reached acceptably low values with respect to the size and number of the NOE violations and the value of the error function describing the geometry. More than 99% of the restraints was satisfied within 0.2 Å. No violation was larger than 1 Å, and no structure had more than 2 violations above 0.5 Å. The average number of violations of the final 17 structures is shown in Figure 3. The rmsd on Cα positions after superposition on the Cαs of residue 3–103 was 1.1 Å. A backbone trace of the final set of structures is given in Figure 4.

Discussion

Enzyme IIB^{cel} consists of a central four-stranded parallel β-sheet, flanked by two and three α-helices on either side, as depicted in Figure 5. The order of the β-strands is 2134. The recently solved X-ray structure of the same enzyme (R.L.M. Van Montfort, T. Pyning, K.H. Kalk, J. Reizer, M.H. Saier, Jr., M.M.G.M. Thunnissen, G.T. Robillard, & B.W. Dystra, in press [1997, *Structure*]) confirms these results. The active site cysteine 10, which is phosphorylated during the catalytic cycle in the wild-type enzyme (Ser 10 in this mutant), is located at the end of the first β-strand just before a loop which is not well defined in the current set of NMR structures. Presumably, this loop (P-loop) provides ligands for the phosphoryl group in the phosphorylated protein. The first α-helix

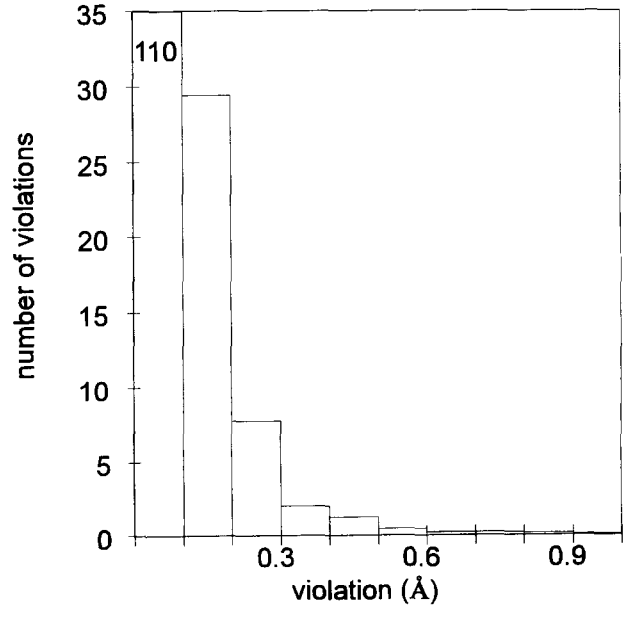

Fig. 3. Upper-bound violations averaged over the set of 17 structures. There are 116 violations lower than 0.1 Å.

Table 1. *Side-chain ^{1}H, ^{15}N and ^{13}C chemical shifts[a] of IIB^{cel} of E. coli in TG-buffer pH = 6.2, 20°C. Tentative assignments are in italics*[b]

	β	γ	δ	ϵ	ζ/η
1met	2.10,2.10(32.77)	2.59,2.52(30.30)		−(−)	
2glu	1.99,1.88(30.26)	2.32,2.24(36.00)	(183.96(CO))		
3lys	1.54,1.33(33.90)	1.46,1.02(26.07)	1.44,1.44(29.30)	2.88,2.88(41.90)	
4lys	1.51,1.75(33.88)	1.64,1.64(29.30)	1.40,1.59(28.43)	2.89,2.89(42.00)	
5his	2.97,2.45(30.63)		7.08(118.99)	*8.44(137.58)*	
6ile	1.92(38.63)	1.38,0.82(28.33)	0.59(14.13)		
		0.65(17.00)			
7tyr	**2.98,2.73**(40.08)		6.98(131.13)	6.82(118.68)	
8leu	**1.40,1.20**(44.78)	1.66(30.40)	0.72(25.80)		
		0.72(27.10)			
9phe	**2.73,2.62**(40.85)		7.26(131.09)	6.88(132.55)	6.74(127.99)
10ser	4.05,3.52(64.94)				
11ser	3.85,4.03(63.57)				
12ala	1.37(18.97)				
14met	2.56,2.11(31.86)	2.60,2.13(−)		−(−)	
15ser	3.95,3.86(62.30)				
16thr	4.24(68.43)	1.08(23.47)			
17ser	*3.99,3.99(62.10)*				
18leu	1.66,1.57(41.54)	1.60(26.70)	0.88(24.00)		
			0.90(24.00)		
19leu	1.93,1.44(40.82)	1.36(26.90)	0.91(27.10)		
			0.63(22.30)		
20val	2.08(31.34)	0.89(24.60)			
		0.70(20.70)			
21ser	4.01,4.11(62.20)				
22lys	2.10,1.95(32.12)	*1.72,1.61(25.16)*	*1.82,1.82(28.51)*	3.02,3.02(42.10)	
23met	2.25,2.09(35.44)	2.81,2.77(32.60)		1.73(15.97)	
24arg	1.89,1.89(30.44)	1.79,1.78(28.53)	3.13,3.02(43.99)	6.66(84.54)	6.88(Hη21)
25ala	1.56(18.12)				
26gln	2.27,1.92(27.62)	2.13,2.27(35.50)		**6.78,7.47**(111.92)	
27ala	1.50(17.56)				
28glu	2.08,2.08(29.49)	2.37,2.20(36.24)			
29lys	1.69,1.70(32.45)	1.03,0.45(24.10)	1.45,1.45(29.10)	2.79,2.76(41.83)	
30tyr	3.32,2.52(38.30)		7.29(133.18)	6.95(118.29)	
31glu	2.14,2.08(26.98)	2.12,2.12(36.71)			
32val	1.99(32.59)	0.95(21.85)			
		0.89(21.70)			
33pro	2.33,1.90(28.57)	2.09,2.09(27.60)	4.05,3.66(50.88)		
34val	1.82(36.28)	0.68(21.95)			
		0.61(18.66)			
35ile	1.26(40.54)	1.26,0.99(27.52)	0.69(12.89)		
		0.89(17.50)			
36ile	1.53(40.56)	1.42,1.41(28.35)	0.76(15.55)		
		0.83(19.55)			
37glu	1.31,1.33(35.21)	1.92,1.85(35.65)	(184.42(CO))		
38ala	0.99(22.92)				
39phe	**2.37,3.13**(42.63)		6.62(131.84)	6.27(130.88)	6.63(129.40)
40pro	2.51,2.03(32.63)	2.13,2.13(27.50)	3.93,3.86(50.65)		
41glu	2.02,1.89(28.25)	2.43,2.16(35.00)			
42thr	4.31(68.20)	6.05,1.28(22.94)			
43leu	1.75,1.64(42.27)	1.65(27.21)	0.98(25.89)		
			0.81(23.03)		
44ala	0.56(17.18)				
46glu	1.97,1.80(31.01)	2.18,1.98(35.96)			
47lys	1.44,1.18(32.09)	0.97,0.21(24.60)	1.36,1.13(−)	2.59,2.63(−)	
49gln	2.08,1.88(33.20)	2.37,2.37(28.24)		6.88,7.59(111.92)	
50asn	2.95,2.71(39.55)		6.97,7.46(111.82)		
51ala	1.20(20.99)				
52asp	2.62,2.44(43.08)				
53val	2.04(34.05)	0.85(21.50)			
		0.89(21.50)			
54val	2.17(33.14)	0.91(21.60)			
		0.85(21.60)			
55leu	1.80,1.22(44.44)	1.50(27.10)	0.64(25.90)		
			0.72(23.50)		
56leu	1.56,1.39(42.70)	1.55(27.20)	0.73(23.58)		
			0.61(25.30)		

(*continued*)

Table 1. *Continued*

	β	γ	δ	ϵ	z/η
58pro	2.22,1.76(30.99)	1.58,1.45(27.80)	2.86,2.40(49.27)		
59gln	2.20,2.06(27.62)	2.48,2.53(33.77)		**6.42,7.91**(111.57)	
60ile	1.99(37.19)	1.41,0.96(27.00)	0.87(18.10)		
		0.87(15.57)			
61ala	1.52(18.80)				
62tyr	**3.16,2.99**(36.34)		7.10(133.70)	6.92(118.86)	
63met	1.94,1.72(32.94)	2.07,1.62(33.04)		−(−)	
64leu	1.92,1.38(39.28)	1.38(26.80)	0.91(25.35)		
			0.76(24.20)		
65pro	2.26,1.86(30.40)	2.11,1.98(28.20)	3.69,3.58(49.05)		
66glu	2.07,1.93(29.42)	2.26,2.26(35.60)			
67ile	1.73(35.82)	1.32,1.12(28.60)	0.44(10.97)		
		0.65(18.30)			
68gln	2.09,1.88(28.71)	2.40,2.40(32.99)		**7.07,7.30**(113.19)	
69arg	1.90,1.84(30.20)	1.71,1.52(27.70)	3.20,3.14(43.00)	7.49,83.49	
70leu	1.80,1.45(43.35)	1.74(26.50)	0.78(23.00)		
			0.75(24.98)		
71leu	1.71,0.98(41.88)	1.34(25.61)	0.68(22.80)		
			0.63(26.86)		
72pro	2.22,1.89(31.80)	1.96,1.86(27.20)	3.53,3.37(50.00)		
73asn	2.90,2.90(37.88)		**7.05,7.61**(113.20)		
74lys	1.70,1.38(33.04)	1.22,1.23(24.20)	1.58,1.45(27.98)	3.22,2.89(42.50)	
75pro	2.29,1.96(31.03)	2.35,1.97(27.50)	3.87,3.66(50.80)		
76val	1.82(33.73)	0.74(20.50)			
		0.62(22.16)			
77glu	2.00,1.60(34.02)	1.99,1.99(35.25)			
78val	1.92(32.43)	0.99(23.00)			
		0.95(21.40)			
79ile	1.50(39.35)	1.70,1.70(29.30)	0.82(13.66)		
		1.19(18.55)			
80asp	2.81,2.49(43.50)				
81ser	*3.93,3.91(62.30)*	—			
82leu	1.84,1.66(40.90)	1.63(27.10)	0.94(24.50)		
			0.87(23.80)		
83leu	1.87,1.45(41.63)	1.93(26.90)	0.90(22.50)		
			0.82(25.30)		
84tyr	3.05,2.87(39.21)		6.93(133.66)	6.69(117.52)	
86lys	1.89,1.73(32.47)	1.57,1.51(24.90)	1.64,1.64(28.90)	2.90,2.90(41.70)	
87val	2.42(28.96)	0.80(24.20)			
		0.70(20.50)			
88asp	2.95,2.29(39.41)				
90leu	1.93,1.48(40.84)	1.43(26.80)	0.90(22.50)		
			0.90(25.30)		
92val	1.93(31.75)	1.04(24.29)			
		0.99(22.10)			
93leu	2.18,1.42(42.16)	2.05(36.80)	0.82(25.82)		
			0.80(24.10)		
94lys	1.81,1.76(32.35)	1.59,1.26(25.90)	1.53,1.53(29.50)	2.78,2.71(41.40)	
95ala	1.50(17.00)				
96ala	1.50(19.04)				
97val	2.04(31.64)	0.90(22.70)			
		0.91(21.20)			
98ala	1.45(17.70)				
99ala	1.45(18.26)				
100ile	1.94(38.15)	1.89,0.65(29.10)	0.67(13.45)		
		0.85(17.10)			
101lys	1.84,1.84(32.38)	1.54,1.40(25.10)	1.62,1.62(29.00)	2.90,2.90(41.70)	
102lys	1.87,1.87(32.50)	1.48,1.43(24.90)	1.67,1.67(29.10)	2.94,2.94(−)	
103ala	1.46(18.78)				
104ala	1.42(19.01)				
105ala	1.40(19.09)				
106asn	2.74,2.65(40.32)		**6.82,7.51**(112.70)		

[a]The ^{1}H chemical shifts are relative to TSP, the ^{15}N chemical shifts are relative to liquid NH_3 (Live et al., 1984), and the ^{13}Ca and ^{13}CO chemical shift are relative to hypothetical internal TSP (Bax & Subramanian, 1986).

[b]Stereochemically assigned shifts are in bold. The estimated error in the chemical shifts is ±0.01 ppm for ^{1}H, and ±0.2 ppm for ^{15}N and ^{13}C. The chemical shifts of heteroatoms are given between parentheses. Missing assignments are indicated by a minus (−) sign.

Table 2. *H-bond restraints used during the structure determination and refinement*[a]

Donor H	Acceptor O	Donor H	Acceptor O
4lys	33pro	53val	5his
6ile	35ile	54val	75pro
7tyr	53val	55leu	7tyr
8leu	37glu	56leu	77glu
9phe	55leu	57gly	9phe
10ser	39phe	67ile	63met
20val	16thr	68gln	64leu
21ser	17ser	69arg	65pro
22lys	18leu	70leu	66glu
23met	19leu	77glu	54val
24arg Hε	36ile	79ile	56leu
24arg	20val	84tyr	80asp
25ala	21ser	85gly	81ser
26gln	22lys	86lys	82leu
27ala	23met	87val	83leu
28glu	24arg	94lys	90leu
29lys	25ala	95ala	91gly
35ile	4lys	96ala	92val
37glu	6ile	97val	93leu
39phe	8leu	98ala	94lys
47lys	43leu	99ala	95ala
48gly	44ala	100ile	96ala
49gln	45gly	101lys	97val
50asn	46glu	102lys	98ala
51ala	47lys	103ala	99ala

[a]If a side-chain atom is involved in an H-bond, this is indicated in the table.

follows the P-loop, pointing with its N-terminal side towards the P-loop where its α-helix dipole (Hol, 1985) could stabilize the negatively charged phosphoryl group. The region behind the first helix, from residue 27 to 34 is also relatively poorly defined (see Fig. 4, 6). If one compares the number of restraints per residue (Fig. 6A) with the rmsd on backbone atoms (Fig. 6B), one sees that the disorder in the P-loop is clearly due to a lack of restraints in this area. For the region around residue 27–34 this is not the case, since both the number of restraints (Fig. 6) and the size and number of violations (Fig. 7) are relatively high for this region. This behavior might be due to conformational averaging, which will be investigated using time-averaged restrained MD simulations (Torda et al., 1989).

The NMR backbone assignment of the IIB domain of another PTS transporter, EII^{glc}, was published by Golic Grdadolnik et al. (1994). The catalytic cysteine is, as in IIB^{cel}, positioned at the end of a β-strand. However, in contrast with the topology of IIB^{cel}, IIB^{glc} consists of a four-stranded antiparallel β-sheet and three α-helices.

The low-molecular-weight PTPase from bovine heart (Su et al., 1994) has a topology resembling that of IIB^{cel}. This PTPase contains an extra α-helix following the second β-strand and a long loop after the fourth β-strand. Also, the *Yersina* PTPase (Stuckey et al., 1994) contains an α/β motif similar to that of IIB^{cel}, with a cysteine at the end of the β-strand. The overall topology is nevertheless different.

The active-site environment of the mean structure is depicted in Figure 8. The current conformations of the P-loop still allow ample speculation about the nature of phosphoryl-group binding. Since there are no positively charged residues in the vicinity of the active site, polar groups will probably be responsible for binding the phosphoryl-group. The crystal structure of the *Yersina* PTPase complexed with a tungstate (WO_4^{2-}) transition-state analog in the active site suggested that in the PTPase the backbone amide hydrogens of the P-loop act as ligands for the phosphoryl-group. Possibly the same situation exists in phospho-IIB^{cel}. Another possibility arises from the high proportion of hydroxyl-containing residues close to the active site, i.e., Ser 11, Ser 15, Thr 16, Ser 17, Ser 81, and Tyr 84, of which the last four are either conserved or similar between the mannitol and the cellobiose IIB sequences. The hydroxyl groups of these residues could also function in binding the phosphoryl group. Yet another possibility is that they are involved in interaction with IIA^{cel}

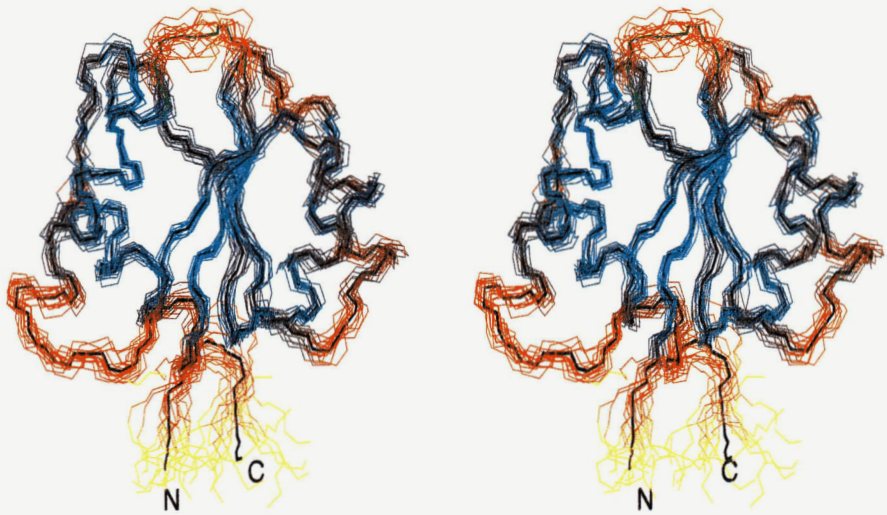

Fig. 4. Stereo picture of the backbone trace of the cluster of 17 IIB^{cel} structures. The traces are colored from blue (low rmsd) via red to yellow (high rmsd). The thick trace in black and green (residues 11–15) represents the trace according to the mean coordinates. The picture was made using MOLMOL (Koradi et al., 1996).

Fig. 5. Cartoon picture of IIB^{cel}. α-helices are shown in red/yellow, β-sheets in cyan, loops in grey. The picture was made using the program MOLMOL (Koradi et al., 1996).

or IIC^{cel} or even with cellobiose, although there is no report of direct interaction of the carbohydrate with an isolated IIB domain.

The B-domain of EII^{mtl} possesses only one tyrosine, that corresponding to Tyr 84 in IIB^{cel}. Fluorescence measurements suggest that this tyrosine in IIB^{mtl} is ionized down to pH 6 (Meyberg et al., 1996). Tyrosinate fluorescence is more difficult to observe in IIB^{cel} because it is masked by a normal tyrosine fluorescence signal from other tyrosines in the enzyme. The position of Tyr 84 in IIB^{cel} and the unusual ionization properties of the equivalent residue in the B-domain of EII^{mtl} may be pointing to a special role for this residue in the catalytic mechanism.

Materials and methods

Sample preparations

Unlabeled, uniformly ^{15}N-labeled and uniformly $^{15}N,^{13}C$-labeled material was produced and purified as described by AB et al. (1994). All samples were in 20 mM Tris-Acetate pH = 6.18, 100 mM NaCl, 3% deuterated (D5) Glycerol. The protein concentrations in the unlabeled, ^{15}N-labeled, and $^{15}N,^{13}C$-labeled samples were 3 mM, 4 mM, and 2mM, respectively. Glycerol was exchanged for deuterated (D5) glycerol by repeatedly diluting and concentrating the sample with buffer containing deuterated glycerol.

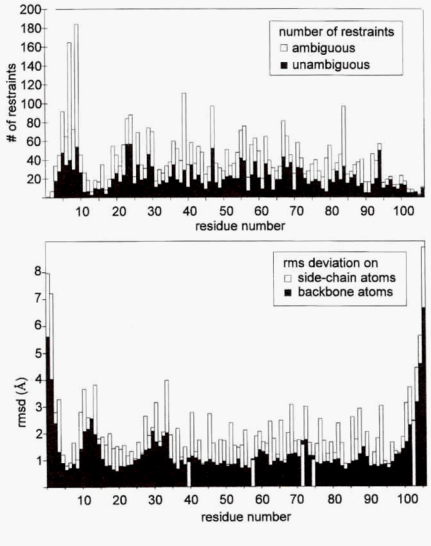

Fig. 6. A: Number of restraints for each residue, used to calculate the final set of 17 structures. Black bars and white bars represent unambiguous and ambiguous restraints, respectively. **B:** Average pairwise root-mean-square deviation for backbone atoms (black bars) and heavy side-chain atoms (white bars) after superposition of the set of 17 structures on Cα 3–103.

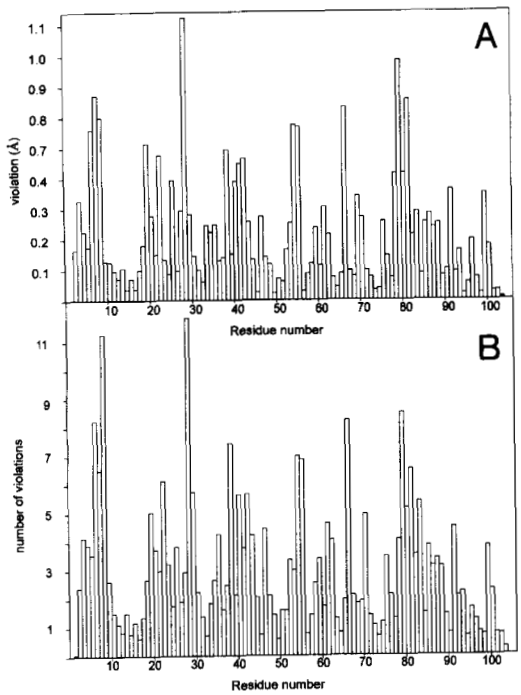

Fig. 7. Summary of the upper-bound violations in the set of 17 structures. **A:** Sum of violations for each residue. **B:** Number of violations for each residue.

NMR spectroscopy

If not mentioned otherwise, the experiments were performed on a Varian Unity 500 MHz NMR spectrometer. All spectra were recorded at 20 °C.

The ^{15}N-NOESY-HSQC and ^{15}N-TOCSY-HSQC (Marion et al., 1989; Zuiderweg & Fesik, 1989; Fesik & Zuiderweg, 1990) were performed as described previously (AB et al., 1994).

Experimental details for the NMR experiments are listed in Table 3.

A series of 2D NOE spectra with mixing times of 40, 60, 100, and 150 ms was performed on a Varian 750 MHz spectrometer (Bijvoet Center, University of Utrecht, NL), using unlabeled protein in H_2O. The water resonance was suppressed by presaturation for 1 s. During the mixing time, unwanted coherences were reduced by applying a homospoil pulse. In the 40 ms mixing time the homospoil pulse was not applied because the recovery time of the homospoil was longer than the mixing time.

Pulsed field gradients along the Z-axis were used to improve the HCCH-TOCSY, the HCCH-COSY, the COCCH-TOCSY, and the HCH experiment in the following manner: When the desired magnetization was present as longitudinal spin order during the INEPT and reversed INEPT steps, a gradient pulse was inserted. Gradient pulses were also applied on both sides of π pulses to reduce artifacts caused by pulse imperfections (Bax & Pochapsky, 1992).

For conversion of the 2D NOE intensities into distance-restraints, we used the Hδ–Hϵ distances in aromatic residues (2.5 Å) and sequential αN (i, i + 1) distances in the β-sheet region (2.2 Å). The height of the peak maxima (m) in the 60 ms 2D NOE experiment was converted to upper limit distance restraints (ul) using the formula: $ul = f(1/m)^{1/6}$. The conversion factor (f) was chosen in such a way that it was as low as possible but so that none of the reference intensities yielded an upper limit distance restraint that was smaller than the actual distance.

Structure calculations

The 3D ^{13}C -HSQC-NOESY, the 3D ^{15}N-NOESY-HSQC, and the 60 ms 2D NOESY experiments yielded 598 unambiguous NOE distance restraints for the first round of structure calculations. All NOEs were interpreted equally as distance bounds of 5 Å. The secondary structure information available from the backbone assignment was used to define 50 hydrogen bond restraints. In the H-bond restraints, the distance between the oxygen and the nitrogen was restrained to be between 2.5 Å and 3.5 Å, and the distance between the hydrogen and oxygen was restrained to be between 1.5 Å and 2.5 Å.

The upper and lower distance bounds were collected in a matrix and additional bounds were calculated using triangular inequalities. This smoothed bounds matrix was reduced to the submatrix containing all non-hydrogen atoms, and the amide and α protons. Four-dimensional coordinates were calculated from this matrix with the EMBED algorithm (Crippen & Havel, 1978; Van Nuland et al., 1992).

In order to impose the proper chirality on asymmetric carbons and to insure the proper handedness of α-helices, we used the procedure described by Van Nuland et al. (1992), where the distance restraints are applied to the 4D coordinates and chiral restraints only to the three coordinates corresponding to the three largest radii of inertia of the 4D structures. The error function constructed with these restraints was subjected to conjugate-gradient minimization (300 steps), followed by simulated annealing using the distance bounds driven dynamics approach (DDD) (Kaptein et al., 1988; Scheek et al., 1989), with 1000 steps at 1000 K, after which 1000 steps were performed with temperature coupling to an external bath of 1 K. (Berendsen et al., 1984). The 4D coordinates were projected into 3D space by calculating the coordinates corresponding to the three largest radii of inertia. These 3D coordinates were subjected to further conjugate–gradient optimization and DDD calculation, using the same error function in a similar protocol as described above. Twenty structures were calculated, of which one appeared to have a fold which was inverted relative to the rest of the structures. The other 19 structures were used for further refinement and NOE assignments.

From this point on, distance restraints from the 2D NOE experiment, calibrated as described above, were used. Further refinement was done using an iterative procedure, in which assignments of NOE peaks were alternated with structure calculations. In the first cycles we discarded possible assignments for NOE-peaks if they represented a distance of more than 12 Å in every structure. In subsequent cycles, as the structure cluster became better defined, this distance was gradually decreased to 7.5 Å in the final stages. NOEs that could be assigned to proton pairs showing distances within 5 Å in at least one of the structures were added to the restraints list. First, only unambiguous restraints were added to the list; later, ambiguous restraints were also added, allowing more than one pair of protons to satisfy the restraint (Nilges, 1993).

The structure calculation cycles typically started with an embedding step, followed by repeated rounds of DDD calculations, to improve sampling of conformational space. The DDD runs typically consisted of 1000 steps of MD at 1000 K followed by an annealing step to 1 K in 1000 steps. NOE analysis was performed between the DDD calculations. In the final annealing step, the

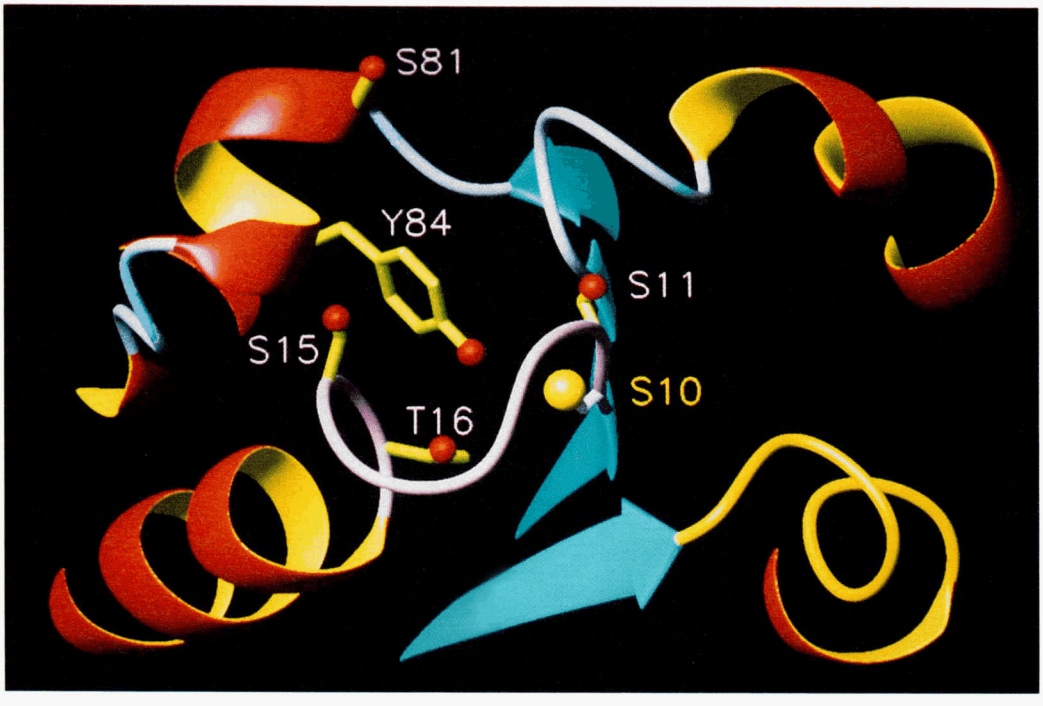

Fig. 8. Cartoon representation of the active-site region of IIB^{cel}. Side-chain hydroxyl groups in the vicinity of the active site are colored red. The hydroxyl-oxygen in S10, a sulfur in the wild type enzyme, is colored in yellow. Backbone trace of residue 11-16 is colored in magenta. Coordinates of the mean structure were used. (Picture was made using MOLMOL (Koradi et al., 1996).)

experimental constraints were given a five times lower weight than the holonomic constraints to prevent restraining forces from causing distortions in the structure. The atomic models of the structures for the MD calculations were gradually extended to include all side-chain hydrogens as explicit atoms. Pseudo-atoms were only used for the methyl protons. Distance restraints including methyl protons were loosened by 0.3 Å for every methyl atom in the restraint (Koning et al.,1990).

Non-equivalent methyl groups of Val and Leu as well as Gly Hα's were treated in the first cycles by the method of flipping chiralities, as described by Van Nuland et al. (1992). In the final cycles all these cases were treated using ambiguous distance restraints. With ambiguous distance restraints, a NOE is considered to be the sum of all the NOEs between the pairs of protons which constitute possible assignments of that NOE. If the sum of these NOEs is violated in the MD calculation, a restraining force is applied, equally distributed over all pairs. This method is well suited to prevent large pseudo-atom corrections in the case of aromatic ring protons, but it can also be used to include NOE information in the structure calculation before the NOE is definitively assigned to one specific pair of protons. If both partners of non-equivalent methyl groups or methylene protons were involved in identical restraints with different bounds, they were treated as follows. Both restraints were kept in the restraint list with the least restrictive bound of the two. To be even more restrictive, the intensity of the two NOEs giving rise to the individual restraints were added and an ambiguous upper distance bound in accordance with this summed NOE was applied to both pairs of protons.

For example, in the two following (hypothetical) restraints, the Hα1 and Hα2 are not stereospecifically assigned; the indices 1 and 2 correspond to the higher and lower chemical shift, respectively:

1. 12ala H^N—13gly Hα1 upper limit: 4.0 Å
2. 12ala H^N—13gly Hα2 upper limit: 3.0 Å.

They can be translated to the following set of one ambiguous and two unambiguous restraints:

1. 12ala H^N—13gly Hα1 upper limit 4.0 Å
2. 12ala H^N—13gly Hα2 upper limit 4.0 Å
3. 12ala H^N—13gly Hα1
   12ala H^N—13gly Hα2 upper limit 2.9 Å.

For the combined ambiguous restraint (3), the upper limit is calculated as follows:

$$d' = \left(\sum d_i^{-6}\right)^{-1/6}$$

where d_i = upper limit distance of the original restraint i

d' = (hypothetical) upper limit "distance" corresponding to the sum of the observed NOEs.

For the final structure calculations, 1961 NOE intensities were used to generate restraints, of which 1319 were uniquely assigned. NOE intensities involving unequivalent protons of both methylene groups and methyl groups of Val and Leu residues were interpreted as combined ambiguous restraints as described above. NOE intensities involving equivalent protons of aromatic rings and of methyl groups were interpreted as ambiguous restraints to explicit protons. This yielded a total of 2129 restraints.

Thirty-two structures were embedded in the last round of structure calculations, using the final set of restraints, which were all subjected to DDD refinement.

Table 3. *NMR-experiments used for the side-chain assignments and structure determination of IIB^{cel}*

Experiment	Nucl.	Spectral width[a] (kHz)	Carrier[b] (ppm)	Maximum evolution time (ms)	Method	References/Remarks
CBCACOHA	$^{13}C\alpha\beta$	10.0	45.844	7.15	TPPI	Kay (1993)
	$^{13}C'$	2.5	175.527	25.6	TPPI	
	^{1}H	8.0	4.813	128		
CBCA(CO)NH	$^{13}C\alpha\beta$	10.0	45.843	6.4	TPPI	Grzesiek & Bax (1992)
	^{15}N	2.0	116.702	32	TPPI	
	^{1}H	7.0	4.813	73.14		
HBHA(CBCACO)NH	$^{13}C\alpha\beta$	5.0	4.813	12.8	TPPI	Grzesiek & Bax (1993a)
	^{15}N	2.0	116.702	22.5	TPPI	
	^{1}H	7.0	4.813	73.14		
HCCH-TOCSY	^{1}H	4.0	2.517	18.75	TPPI	Olejniczak et al. (1992)
	^{13}C	10.0	44.88	7.5	TPPI	
	^{1}H	8.0	2.517	256		
HCCH-TOCSY aromats	^{1}H	3.5	6.563	18.3	TPPI	Olejniczak et al. (1992); Kay et al. (1993)
	^{13}C	10.0	130.97	7.5	TPPI	
	^{1}H	3.5	26.563	146.3		
HCCH-COSY	^{1}H	4.0	2.517	16	TPPI	Ikura et al. (1991)
	^{13}C	10.0	44.88	6.6	TPPI	
	^{1}H	8.0	2.517	128		
HCH	^{1}H	4.0	2.812	48	TPPI	Yamazaki et al. (1993)
	^{13}C	3.333	53.799	28.8	TPPI	
	^{1}H	4.0	2.812	128		
COCCH-TOCSY	^{13}C	5.0	58.174	6.4	TPPI	AB et al. (in preparation)
	$^{13}C'$	2.5	177.51	16	TPPI	
	^{1}H	7.0	4.813	73.1		
2D NOE buildup	^{1}H	20.0	4.813	30	States	Tmix: 40, 60, 100, 150 ms
	^{1}H	10.0	4.813	419.6		
3D ^{13}C-HSQC-NOESY	^{1}H	7.0	4.813	18.3	TPPI	Majumdar & Zuiderweg (1993)
	^{13}C	10.0	44.89	6.4	TPPI	Tmix: 100 ms
	^{1}H	7.0	4.813	73.1		

[a]The spectral domains are in the order $\omega1,\omega2$, ($\omega3$).
[b]The carrier position is given in ppm relative to TSP for ^{1}H and ^{13}C, and relative to liquid NH_3 for ^{15}N.

The coordinates were deposited at the PDB under accession number 1E2B.

Acknowledgments

We thank Karl Hård and Rolf Boelens at the Bijvoet Center in Utrecht for their help and the measurement time on the Varian 750 MHz spectrometer. We thank Frans van Hoesel for writing the program SNARF, which was used for all data processing and analysis of NMR spectra. We thank Varian for supplying us with the triple-resonance gradient probe.

References

Ab E, Schuurman-Wolters GK, Saier MH, Reizer J, Jacuinod M, Roepstorff P, Dijkstra K, Scheek RM, Robillard GT. 1994. Enzyme IIB-cellobiose of the phosphoenol-pyruvate-dependent phosphotransferase system of *Escherichia coli*: Backbone assignment and secondary structure determined by three dimensional NMR spectroscopy. *Protein Sci 3*:282–290.

Bax A, Pochapsky SS. 1992. Optimized recording of heteronuclear multi-dimensional NMR spectra using pulsed field gradients. *J Magn Reson 99*:638–643.

Bax A, Subramanian S. 1986. Sensitivity-enhanced two-dimensional heteronuclear shift correlation NMR spectroscopy. *J Magn Reson 67*:565–569.

Berendsen HJC, Postma JPM, DiNola A, Haak JR. 1904. Molecular dynamics with coupling to an external bath. *J Chem Phys 23*:3684–3690.

Cho H, Krishnaraj R, Kitas E, Bannewarth W, Walsh CT, Anderson KS. 1992. Isolation and structural elucidation of a novel phosphocysteine intermediate in the LAR protein tyrosine phosphatase enzymatic pathway. *J Am Chem Soc 114*:7296–7298.

Crippen GM, Havel TF. 1978. Stable calculation of coordinates from distance information. *Acta Crystallographica A34*:282–284.

Fesik SW, Zuiderweg ERP. 1990. Heteronuclear three-dimensional NMR spectroscopy of isotopically labeled macromolecules. *Q Rev Biophys 23*:97–131.

Golic Grdadolnik S, Eberstadt M, Gemmecker G, Kessler H, Buhr A, Erni B. 1994. The glucose transporter of *Escherichia coli*. Assignment of the ^{1}H,^{13}C, and ^{15}N resonances and identification of the secondary structure of the soluble IIB domain. *Eur J Biochem 219*:945–952.

Grzesiek S, Bax A. 1992. Correlating backbone amide and side chain resonances in larger proteins by multiple relayed triple resonance NMR. *J Am Chem Soc 114*:6291–6293.

Grzesiek S, Bax A. 1993a. Amino acid type determination in the sequential assignment procedure of uniformly carbon-13/nitrogen-15-enriched proteins. *J Biomol NMR 3*:185–204.

Grzesiek S, Bax A. 1993b. The importance of not saturating water in protein NMR. Application to sensitivity enhancement and NOE measurements. *J Am Chem Soc 115*:12593–12594.

Guan K, Dixon JE. 1991. Evidence for protein-tyrosine-phosphatase catalysis

proceeding via a cysteine-phosphate intermediate. *J Biol Chem 266*:17026–17030.

Hol WGJ. 1985. The role of the α-helix dipole in protein function and structure. *Prog Biophys Mol Biol 45*:149–195.

Ikura M, Kay LE, Bax A. 1991. Improved three-dimensional ^{1}H-^{13}C-^{1}H correlation spectroscopy of a ^{13}C labeled protein using constant-time evolution. *J Biomol NMR 1*:299–304.

Kaptein R, Boelens R, Scheek RM, Van Gunsteren WF. 1988. Protein structures from NMR. *Biochemistry 27*:5389–5395.

Kay LE. 1993. Pulsed-field gradient-enhanced three-dimensional NMR experiment for correlating $^{13}C_{\alpha/\beta}$, $^{13}C'$, and $^{1}H_{\alpha}$ chemical shifts in uniformly ^{13}C-labeled proteins. *J Am Chem Soc 115*:2055–2057.

Kay LE, Xu GY, Singer AU, Muhandiram DR, Forman-Kay J. 1993. A gradient-enhanced HCCH-TOCSY experiment for recording side-chain ^{1}H and ^{13}C correlations in H_2O samples of proteins. *J Magn Reson Ser B 101*:333–337.

Koning TMG, Boelens R, Kaptein R. 1990. Calculation of the nuclear Overhauser effect and the determination of proton–proton distances in the presence of internal motions. *J Magn Reson 90*:111–123.

Koradi R, Billeter M, Wüthrich K. 1996. MOLMOL: A program for display and analysis of macromolecular structures. *J Mol Graphics 14*:51–55.

Live DH, Davis DG, Agosta WC, Cowburn D. 1984. Long-range hydrogen bond mediated effects in peptides: ^{15}N NMR study of gramicidin S in water and organic solvents. *J Am Chem Soc 106*:1939–1941.

Lolkema JS, Robillard GT. 1992. The Enzymes II of the phosphoenolpyruvate-dependent carbohydrate transport systems. *New Compr Biochem 21*:135–167.

Lolkema JS, Ten Hoeve-Duurkens RH, Swaving-Dijkstra D & Robillard GT. 1991b. Mechanistic coupling of transport and phosphorylation activity by enzyme II^{mtl} of the *Escherichia coli* phosphoenolpyruvate-dependent phosphotransferase system. *Biochemistry 30*:6716-6721

Lolkema JS, Swaving-Dijkstra D, Ten Hoeve-Duurkens RH, Robillard GT. 1991a. Interaction between the cytoplasmic and membrane-bound domains of enzyme II^{mtl} of the *Escherichia coli* phosphoenolpyruvate-dependent phosphotransferase system. *Biochemistry 30*:6721–6726.

Majumdar A, Zuiderweg ERP. 1993. Improved carbon-13-resolved HSQC-NOESY spectra in water using pulsed-field gradients. *J Magn Res Ser B 102*:242–244.

Marion D, Driscoll PC, Kay LE, Wingfield PT, Bax A, Gronenborn AM, Clore GM. 1989. Overcoming the overlap problem in assignment of ^{1}H-NMR spectra of larger proteins by use of three-dimensional heteronuclear ^{1}H–^{15}N Hartmann-Hahn multiple quantum coherence and nuclear-Overhauser multiple quantum coherence spectroscopy: Application to interleukin 1b. *Biochemistry 28*:6150–6156.

Meadow ND, Fox DK, Roseman S. 1990. The bacterial phosphoenol-pyruvate: glucose phosphotransferase system. *Annu Rev Biochem 59*:497–542.

Meins M, Jenö P, Müller D, Richter WJ, Rosenbusch JP, Erni B. 1993. Cysteine phosphorylation of the glucose transporter of *E. coli*. *J Biol Chem 268*:11604–11609.

Meyberg W, Schuurman-Wolters GK, Robillard GT. 1996. Interdomain interactions between the hydrophilic domains of the mannitol transporter of *Escherichia coli* in the unphosphorylated and phosphorylated states. *Biochemistry 35*:2759–2766.

Nilges M. 1993. A calculation strategy for the structure determination of symmetric dimers by ^{1}H-NMR. *Proteins 17*:297–309.

Olejniczak E, Xu RX, Fesik SW. 1992. A 4D HCCH-TOCSY experiment for assigning the side-chain proton and carbon-13 resonances of proteins. *J Biomol NMR 2*:655–659.

Parker LL, Hall BG. 1990. Characterization and nucleotide sequence of the cryptic cel operon of *Escherichia coli* K12. *Genetics 124*:455–471.

Pas HH, Robillard GT. 1988. 3-phosphocysteine and phosphohistidine are intermediates in the phosphoenol-pyruvate dependent mannitol transport catalyzed by *Escherichia coli* EIImtl. *Biochemistry 27*:5835–5839.

Pas HH, Ten Hoeve-Duurkens RH, Robillard GT. 1988. Bacterial phosphoenolpyruvate dependent phosphotransferase system: Mannitol-specific EII contains two phosphoryl binding sites per monomer and one high-affinity mannitol binding site per dimer. *Biochemistry 27*:5520–5525.

Pas HH, Meyer G, Kruizinga WH, Tamminga KS, Van Weeghel RP, Robillard GT. 1991. 31P phospho-NMR demonstration of phosphocysteine as a catalytic intermediate on the *Escherichia coli* phosphotransferase system EIImtl. *J Biol Chem 266*:6690–6692.

Postma PW, Lengeler JW, Jacobson GR. 1993. Phosphoenolpyruvate-carbohydrate phosphotransferase systems of bacteria. *Microbiol Rev 57*:543–574.

Reizer J, Reizer A, Saier MH Jr. 1990. The cellobiose permease of *Escherichia coli* consists of three proteins and is homologous to the lactose permease of Staphylococcus aureus. *Res Microbiol 141*:1061–1067.

Saier MH Jr, Reizer J. 1992. Proposed uniform nomenclature for the proteins and protein domains of the bacterial phosphoenolpyruvate:sugar phosphotransferase system. *J Bacteriol 174*:1433–1438.

Scheek RM, Van Gunsteren WF, Kaptein R. 1989. Molecular dynamics simulation techniques for determination of molecular structures from nuclear magnetic resonance data. *Methods Enzymol 177*:204–218.

Stuckey JA, Schubert HL, Fauman EB, Zhang ZY, Dixon JE, Saper MA. 1994. Crystal Structure of *Yersina* protein tyrosine phosphatase at 2.5 Å and the complex with tungstate. *Nature 370*:571–575.

Su XD, Taddei N, Stefani M, Ramponi G, Nordlund P. 1994. The crystal structure of a low molecular weight phosphotyrosine protein phosphatase. *Nature 370*:575–578.

Torda AE, Scheek RM, Van Gunsteren WF. 1989. Time-dependent distance restraints in molecular dynamics simulations. *Chem Phys Lett 157*:289–294.

Van Nuland NAJ, Grötzinger J, Dijkstra K, Scheek RM, Robillard GT. 1992. Determination of the three dimensional solution structure of the histidine-containing phosphocarrier protein HPr from *Escherichia coli* using multidimensional NMR spectroscopy. *Eur J Biochem 210*:881–891.

Yamazaki T, Yoshida M, Nagayama K. 1993. Complete assignments of magnetic resonances of ribonuclease H from *Escherichia coli* by double- and triple-resonance 2D and 3D NMR spectroscopies. *Biochemistry 32*:5656–5669.

Zuiderweg ERP, Fesik SW. 1989. Heteronuclear three-dimensional NMR spectroscopy of the inflammatory protein C5a. *Biochemistry 28*:2387–2391.